Near-diffraction limited coherent X-ray focusing using planar refractive lenses made of epoxy SU-8 resist

I.Snigireva[1], A. Snigirev[1], M. Drakopoulos[2], V. Kohn[3],
V.Nazmov[4,5], E.Reznikova[4], J.Mohr[4], V.Saile[4,5]

[1]ESRF, BP-220, Grenoble Cedex, France
[2] Diamond Light Source Ltd, Oxfordshire OX11 0QX, U.K.
[3] Russian Research Centre "Kurchatov Institute", 123182 Moscow, Russia
[4] Institut für Mikrostrukturtechnik/Forschungszentrum Karlsruhe GmbH, 76021 Karlsruhe, Germany
[5] University of Karlsruhe, 76128 Karlsruhe, Germany

ABSTRACT

We present results on comprehensive studies of high resolution SU-8 planar refractive lenses. Lens optical properties were investigated using coherent high energy X-ray radiation. Resolution of about 270 nm was measured for the lens consisting of 31 individual lenses at energy 14 keV. Coherent properties of the set-up permit to resolve near-focus fine structure, which is determined by tiny aberrations caused by lens imperfections close to the parabola apex. This study allows understanding as far SR deep lithography as possible can maintaine to close tolerances for lens parameters. Two-dimensional focusing crossed lenses were tested and imaging experiments in projection and imaging mode were conducted. Radiation stability test was performed and conclusions on the applicability of SU-8 lenses were done.

Keywords: Planar refractive lenses, X-ray focusing, imaging, deep lithography

1. INTRODUCTION

Shortly after the first successful demonstration of the applicability of compound refractive lenses for high energy X-ray focusing [1] the use of planar lenses was proposed applying modern micro fabrication technologies including LIGA-like technique [2]. Micro fabrication technology was used to manufacture X-ray lenses from PMMA, SU-8 resist, Si, diamond, glassy carbon and boron [3-22]. Such lenses have been tested at the ESRF and have shown excellent focusing and imaging properties in the energy range from 8 to 100 keV [11-16]. Planar lenses are well suited for high-resolution diffraction experiments including standing wave technique [23-25]. Focusing with planar lenses in the nanometer resolution range is feasible and the lateral focal spot size close to 100 nm was already demonstrated with the use of lenses with very short focal distances [17,19]. In addition, X-ray refractive collimators have been proposed and tested showing a micro- and sub micro-radian collimation [16].

Planar lenses made by microfabrication techniques are one-dimensional or linear optical elements and they are strongly needed and widely used at synchrotron beamlines. Typically a synchrotron source is asymmetric – it is rather smaller vertically compared to horizontal direction, therefore astigmatic focusing is often required to obtain a round spot. This can be achieved with independent horizontal and vertical focusing elements. Linear refractive lenses can be easily combined with other optical elements already mounted at the beamlines such as bent mirrors and crystals. Furthermore linear focusing is needed for many high-resolution diffraction and scattering techniques including – surface analysis, high-resolution diffraction experiments, standing wave technique etc.

It should be pointed out that, microfabrication technologies make possible the formation of planar lens arrays with a wide range of parameters. Lens apertures can range from a few microns to a few millimeters. Structures up to a few mm in depth can be realized. Their focal distances can range from a few millimeters to tens of meters. Planar fabrication techniques can use a broad spectrum of materials from Si, plastics and metals to exotic materials such as diamond.

Among other lens materials SU8 negative epoxy resist is considered to be very promising. According to different literature data SU8 resist is basically composed of low-Z atoms (H, C and O) to the extent of 98% [26]. Because of this, the SU8 epoxy resist was proposed for the direct X-ray lithographic formation of parabolic planar refractive lenses [3, 7-9]. In this paper we present comprehensive studies as far synchrotron radiation deep lithography as possible can maintaine lens parameters. Optical properties of high resolution planar refractive lenses were investigated with hard X-

Design and Microfabrication of Novel X-Ray Optics II, edited by
Anatoly A. Snigirev, Derrick C. Mancini, Proceedings of SPIE Vol. 5539
(SPIE, Bellingham, WA, 2004) · 0277-786X/04/$15 · doi: 10.1117/12.561082

ray coherent radiation. Comparison of the experimental results with computer simulations allows understanding the causes of deviation of focusing from the ideal performance. A new generation of crossed lenses for two-dimensional focusing was fabricated and their focusing and imaging properties were experimentally studied. Results from the radiation stability test are presented. Based upon this examination future perspectives of SU8 refractive lenses are discussed.

2. DIFFRACTION LIMITED RESOLUTIONS

The diffraction-limited resolution is determined as [27]:

$$s_f = 0.47\,\lambda F / A_{eff}, \quad A_{eff} = \left(\lambda F / 2\gamma\right)^{1/2}, \quad F = R / 2N\delta + L/6, \quad \gamma = \beta / \delta$$

Here λ is the wave length of the monochromatic radiation, R is the radius of curvature of parabola, N is number of the bi-concave elementary lenses inside the compound lens, and δ and β are parts of the complex refractive index $n = 1 - \delta + i\beta$ of the lens material. The energy dependence of diffraction-limited resolution for fixed focal distance is shown in Fig. 1a. As shorter the focal distance the better resolution is. The resolution below 250 nm is achievable for medium (around 1m) focal distances, for short focal distances the resolution less then 50 nm can be reached for energy range from 10 to 100 keV. A small presence of Sb in the resist (~1%) deteriorates the resolution above 30 keV due to absorption K-edge.

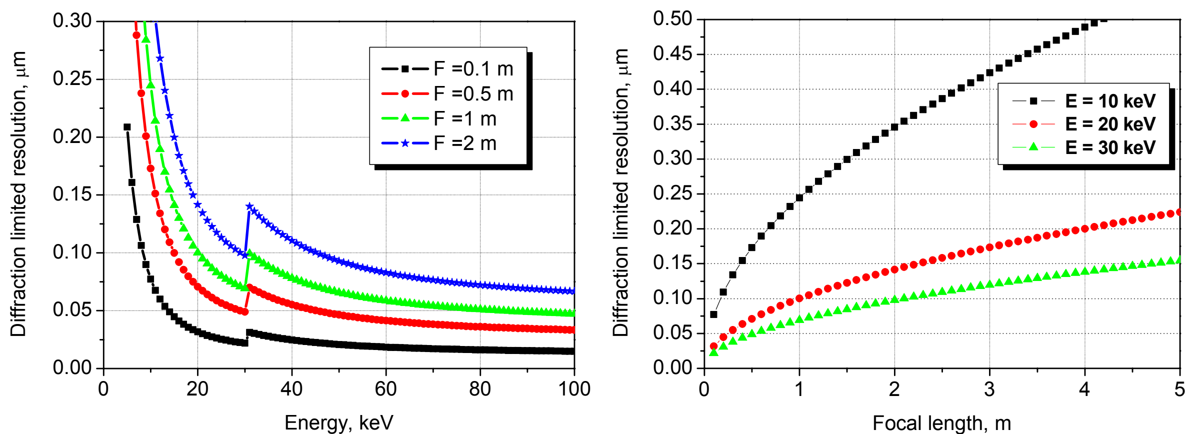

Fig. 1. Graphs showing diffraction limited resolution dependence of energy at fixed focal distances (a) and of focal length at fixed energies (b).

The dependence of the diffraction-limited resolution on the lens focal length at fixed energies is depicted in Fig.1b. It can be seen that the energy increase leads to the resolution improvement and the resolution below 200 nm is easily achievable for energies 20-30 keV for reasonably long focal distances (< 4 m). As an extreme speculation, the resolution of the SU8 lens with a 10 mm focus distance will approach 10 nm at 20 keV.

3. LENS DESIGN AND FABRICATION

The lens fabrication process consists of exposing SU-8 resist layer to synchrotron radiation through a gold working mask of 15-20µm thickness on a 2.7 µm thick titanium membrane stretched over a rigid metal plate. This mask was manufactured by deep X-ray lithography by means of intermediate mask, which was made with electron beam lithography and gold electroplating; the details can be found elsewhere [28-29].

SU8 resist layers with different thickness up to 1mm were coated on a thermally oxidized Si wafer by a casting technique at 95 degrees using a leveled hotplate. In order to obtain the uniform resist thickness and to keep the solvent content of about 2 – 4 %, the pre-exposure baking was carried out. X-ray exposures of SU-8 layers were performed at the LITHO-3 ANKA storage ring beamline with electron energy of 2.5 GeV. The dose distribution in the resist layer from the top to the bottom was varied in the range of 100-40 J/cm^3. The post exposure baking was done in at 95 °C for 30 min for resist cross-linking. Immersion development was carried out without any agitation for the first step and subsequently in acoustically agitated PGMEA-baths and IPA-rinser. After that the drying in an oven at 30 °C was performed. It should be

noted that for all development-rinsing- operations the samples were placed on a special holder with the resist layer downwards. The proposed technology allows to fabricate lenses from the SU-8 resist about 1 mm deep [7,9].

4. 1D LENS CHARACTERIZATION

The focusing properties of 1D lenses were assessed at the ESRF ID18F beamline. For this experiment we used a compound lens consisting of 31 individual lenses. Focal distance was about 23 cm at 14 keV. The full aperture was 320 microns, but the effective aperture was around 100 µm. The radius of parabola tip was 19.7 microns. The spacing between individual lenses was in the order of 7 µm. Linear lenses were arranged to provide focusing in the vertical direction. During the experiments the lens was placed on the translation/rotation stage with 6 degree of freedom. The alignment of the lens was done using a high-resolution X-ray CCD camera.

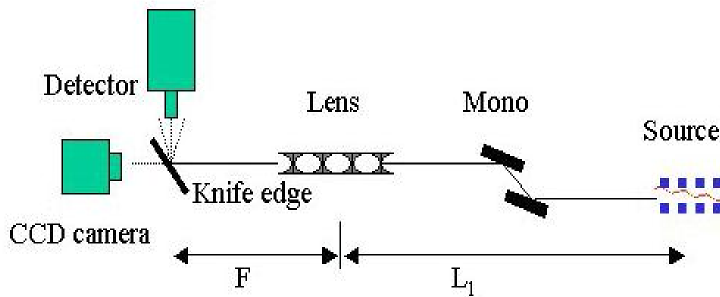

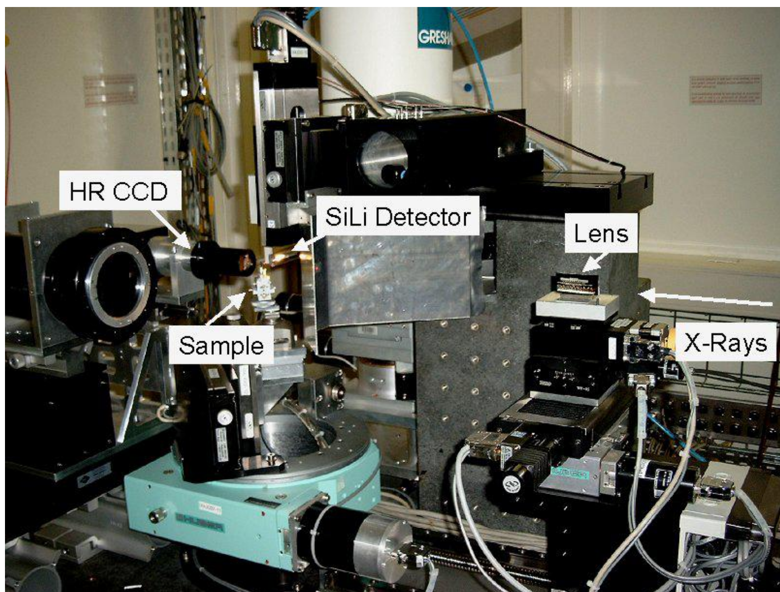

Fig. 2 Sketch (upper part) and photo (in the bottom) of the experimental set-up

An incident X-ray energy of 14 keV was selected by using a cryogenically cooled double crystal Si-111 monochromator. In addition the second crystal was detuned to reduce higher-order harmonic contamination. The lens was placed at a distance L_1 = 59 m from the source. A motorized Huber slit was placed in front of the lens to define the incoming x-ray beam size (Fig. 2). The effective source size measured during the experiment was about 50µm (FWHM) in a vertical direction. The demagnification factor $s = L_1 / F$ was 256; therefore source size limited resolution was in the order of 0.2µm. The diffraction-limited resolution was in the order of 0.1µm.

The lateral size of the microbeam was measured by scanning of a 0.3 µm wide Cu line (Fig. 2) across the beam vertically, recording the fluorescence radiation by an energy dispersive detector. The knife-edge was placed on the stage with required rotation/translation degree of freedom and was aligned with the X-ray camera. Figure 3 shows the copper fluorescence counts as the copper line is scanned through focused X-ray beam in 0.1 µm steps. The focal spot full width at half maximum (FWHM) is 0.4µm. Taking into account the 0.3µm width of copper line, the deconvolved spot size is 0.27 µm. The measured focal spot is in an excellent agreement with calculations and underlines the good lens quality.

The insert in Fig. 3 shows the intensity distribution in the image plane of the lens recorded with the X-ray CCD camera. The focal line is 1 mm long. From the first glance it is quite uniform, but detailed analysis shows that FWHM of the focal line width changes from 0.27 to 1.5 µm. Such changes can be explained by variations of lens geometrical parameters (radius or/and shape of the of parabola). We should mention that the focal depth is about of 0.2 mm for 250 nm resolution and simple estimations show that the shape of the parabola must retain in the depth within 100 nm accuracy (0.1% of the parabola radius).

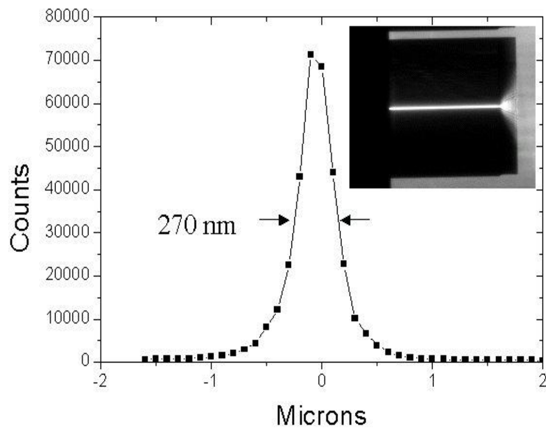

Fig. 3 Vertical scan of the 0.3 µm wide Cu-line as a knife edge through the micro-beam. Insert is the CCD camera image in the lens image plane.

To determine the gain, we have measured Cu fluorescence intensity in the flat and focused beams thorough a 50µm Au-pinhole. The measured gain was about 327 that is in a very good agreement with theoretical calculations.

Knife-edge scans performed for defocused positions at distances 2 mm upstream and 2 mm downstream from the lens focal plane reveal the fine structure of the focused beam (Figure 4). As can be seen at the optimal focusing position the beam profile has almost perfect Gaussian shape. The beam profile consisting of three weak maximums has been taken upstream from the focal plane. Focusing started to split downstream from the focal plane and splitting up to few micrometers was observed. Such behavior is rather usual for some interference phenomena where the coherent superposition of the fields of a different origin lead to increasing or decreasing the intensity due to constructive or destructive interference.

If the lens has some small deviations from the parabolic shape, the Gaussian distribution will be disturbed. To understand the physical nature of this phenomenon we have performed the computer simulations of the X-ray beam focusing by introducing some defects. We have examined the total phase profile of the wave field formed by all elementary lenses in combination with different kinds of objects. As a result of such analysis we came to the conclusion that the real lens consists of two parabolic lenses with different apertures and focal lengths. The main lens has a design radius of curvature of 19.7 µm. The second lens with rather smaller aperture is located at the parabola tip and has the parabola radius of 17.5 µm. Since the aperture of the second lens is much smaller than the first one, the first lens is dominating in the exact focusing position and the contribution of the second lens can be neglected. However, for defocused positions (upstream and downstream from the focal plane) the amplitudes of waves diffracted by various lenses become comparable in amplitude but have different phases. The fine beam structure appears as a result of constructive or destructive interference.

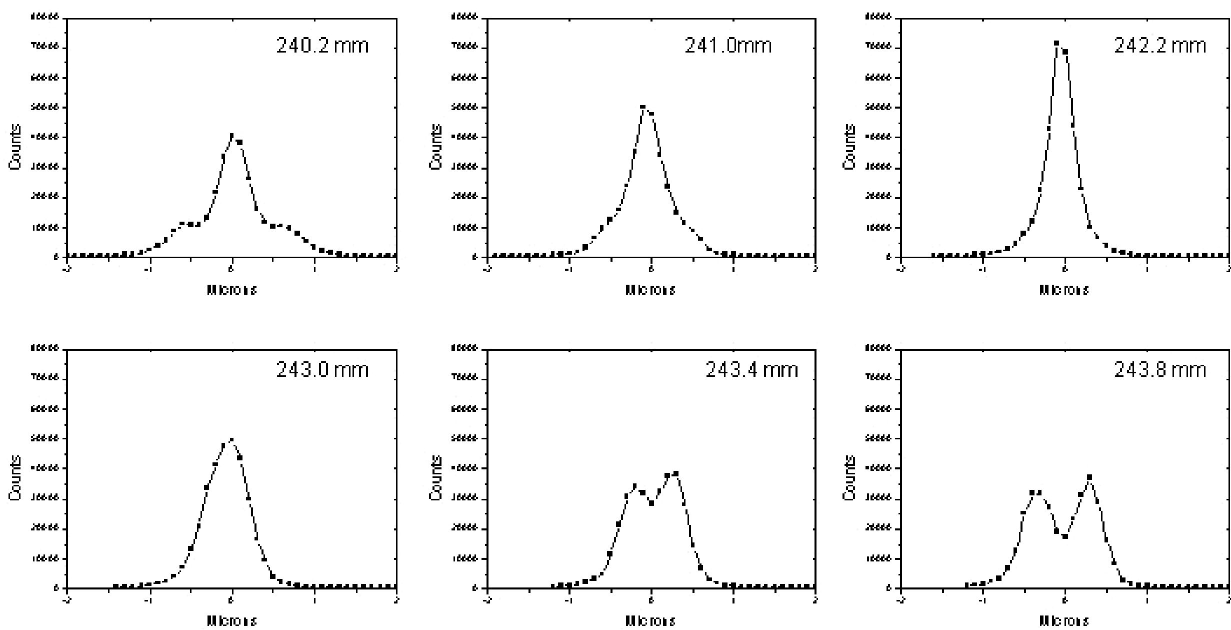

Fig. 4 Vertical scan of the 0.3 µm wide Cu-line as a knife edge through the micro-beam take n at different distances along the optical axis. Focusing was observed at distance 242.2 mm from the lens.

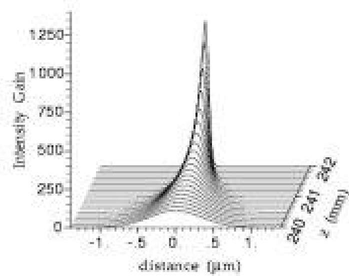

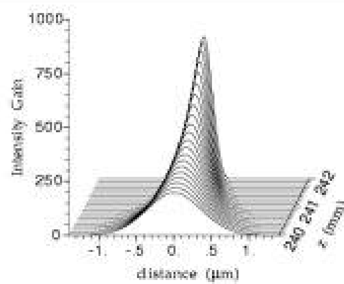

Point source

Extended source

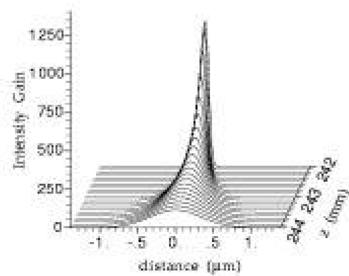

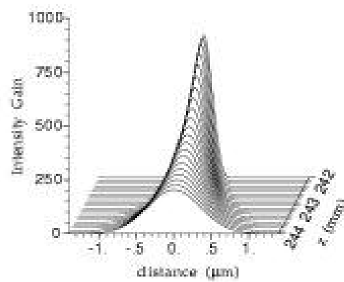

a

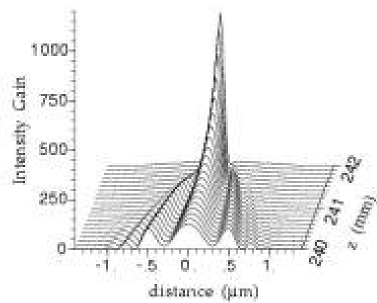

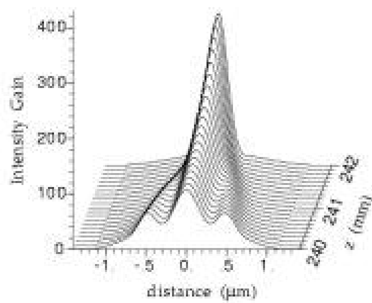

Point source

Extended source

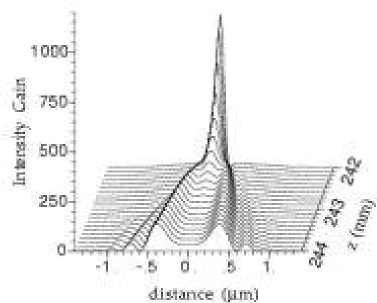

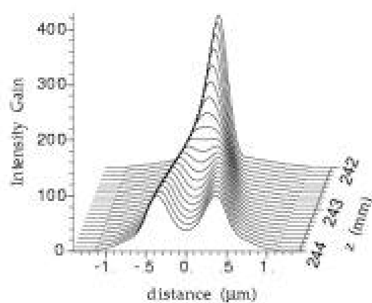

b

The results of calculations of the transverse intensity distribution at the various distances along the optical axis for perfect and slightly aberrated lenses are shown in Fig. 5a and b respectively. The left panel corresponds to the point source and the right one is calculated for the extended source of 60 μm size. We note that for the perfect lens, the source convolution leads only to a wider FWHM without changing of the Gaussian shape. On the contrary, for aberrated lens the convolution with the source size changes essentially fringes shape. This means that the observed interference is not adequate to the interference fringes for the completely coherent illumination. But it can be seen that smoothing the intensity profile over the source size cannot destroy interference fringes. In spite of minor differences the calculated intensity distribution is similar to one measured in the experiment. Thus we can conclude that the physical picture of the interference is determined correctly. It should be mentioned that if the radius of a smaller parabola will be larger then designed one (for example 22.56 μm) the interference picture would be inversed.

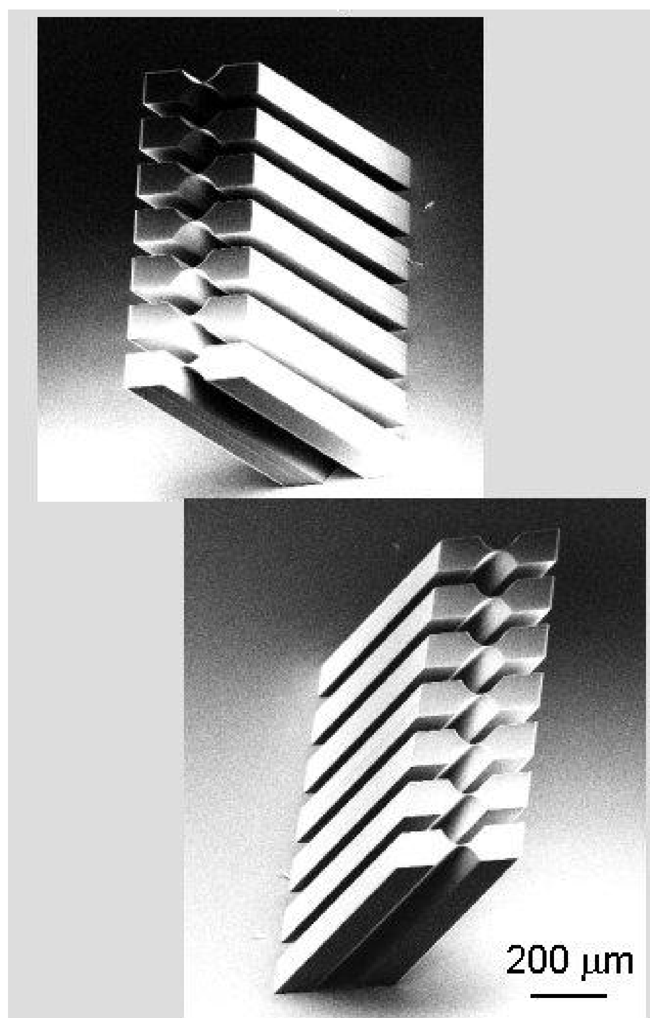

Fig. 6 SEM image of crossed lenses

5. TWO DIMENTIONAL FOCUSING

A new generation of crossed lenses was produced for two-dimensional focusing. These lenses were designed and manufactured at the IMT/FZK. Having regard to the drawbacks of the previous design for two-dimensional lenses [7,9], the working mask was fabricated by means of double exposures tilted at $+45^o$ and$-45\,^o$. The intermediate and working masks were designed and fabricated taking into account the peculiarities of deep X-ray lithography of SU-8 resist layers and optical properties of SU-8 polymer lens. The lenses for vertical and horizontal focusing are separated and lens parameters are defined in the way that each set of lenses has focal distance of about 15 cm for energies from 5 to 30 keV. SEM image of crossed lenses is depicted in Fig. 6. Lens parameters are presented in Table 1.

Table 1. Design parameters of crossed lenses.

	Horizontal focusing, F = 145 mm				Vertical focusing, F = 115 mm			
E, keV	A, μm	R, μm	N	L, μm	A, μm	R, μm	N	L, μm
12.4	120	15.6	29	9096	109	13.9	34	10068
17.5	110	14.2	52	15310	130	17	81	26887
21	78	10.1	53	12380	105	13.8	94	26750
22.2	85	11	64	15856	98	12.8	98	26600

The focusing properties of these lenses were studied in the X-ray energy range from 6 up 30 keV at the BM5 ESRF beamline (see Fig. 7). The X-ray FReLoN CCD camera with the pixel size 0.67 μm and absorption knife edge scans were used for the lens characterization.

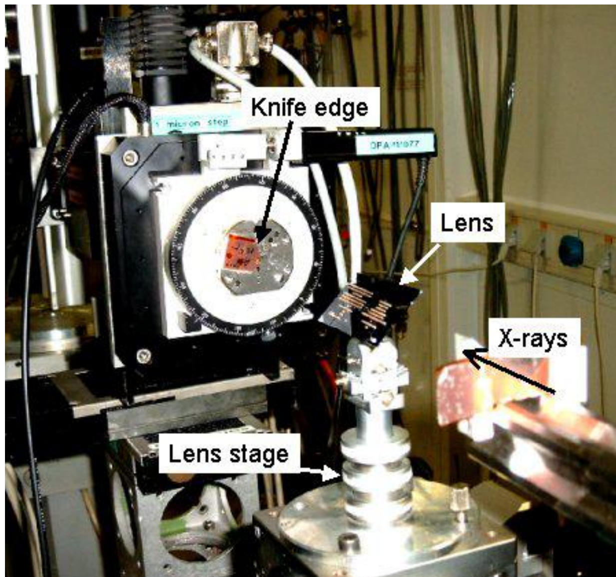

Fig. 7 Photo of experimental setup used for test of crossed lenses at BM 5 beamline

Results of the measured with the X-ray CCD camera of the focal spot and gain are summarized in the Table 2. The camera pixel size was 0.67 μm. Figure 8 (left) shows CCD X-ray image recorded at 17.5 keV in the image plane for the lens consisting of 81vertically and 52 horizontally focusing individual lenses. The measured focal spot was 2.7*2.7 μm^2 in vertical and horizontal directions, respectively. The measured gain was around 380. The intensity knife scan is shown in Fig. 8 (right). The measured FWHM is 1.5 μm.

In order to test imaging properties of two-dimensional lenses two types of experiments were performed. In the first one a scheme as a projection microscope was employed (Fig. 9). A secondary source was generated by lens, and image of Au grid, placed at distance 7 cm from the source, was magnified. The 5-fold magnified image was recorded with the X-ray CCD camera at a distance 35 cm from the lens focus. Figure 9 shows the grid image, when the slits were open up to 1mm. The 2-D magnified image is in the center (see insert). As far as focal distances for vertically and horizontally focusing lenses are slightly different, the divergence is different as well. Vertical lenses have larger divergence and therefore image in vertical direction is lager. Grid images magnified in two directions are surrounded by one-dimensionally magnified images in vertical or horizontal directions. The X-ray image of the grid without magnification is seen as well. The grid pitch size is 12.5 μm.

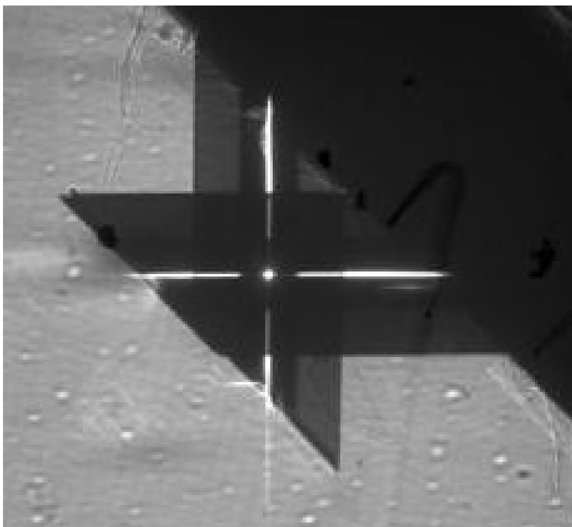

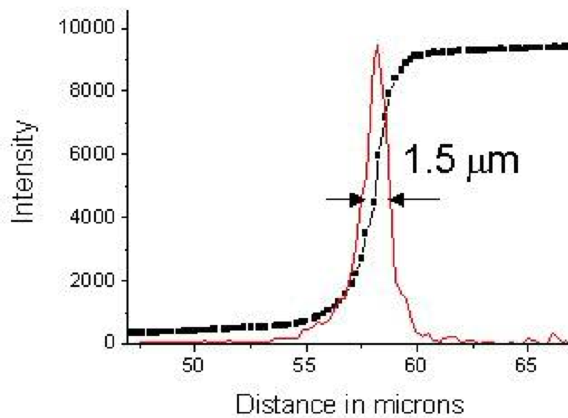

Fig. 8 CCD image recorded at the lens imaging plane (left) and vertical scan of absorption knife-edge through the micro-beam (right)

Table 2. Summary of measured results for SU-8 crossed lenses.

Energy	N vert. lenses	N hor. lenses	Focal distance	FWHM vert	FWHM hor	Gain
12.4 keV	34	29	148 mm	2.2 μm	3 μm	325
17.5 keV	81	52	153 mm	2.7 μm	2.7 μm	390
21 keV	94	53	152 mm	2.4 μm	3 μm	240
22.2 keV	98	64	151 mm	2.2 μm	2.5 μm	380

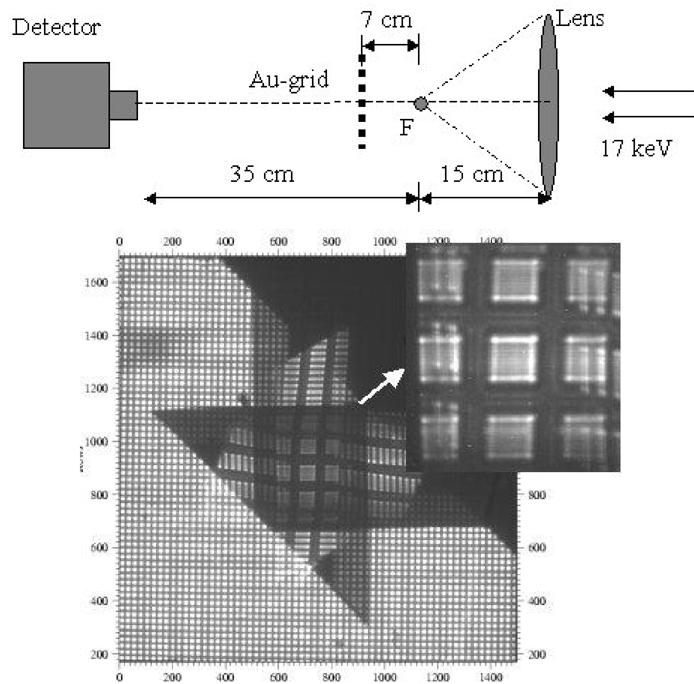

Fig. 9 Experimental setup used for projection microscopy (upper part) and recorded magnified image of the Au grid (at the bottom).

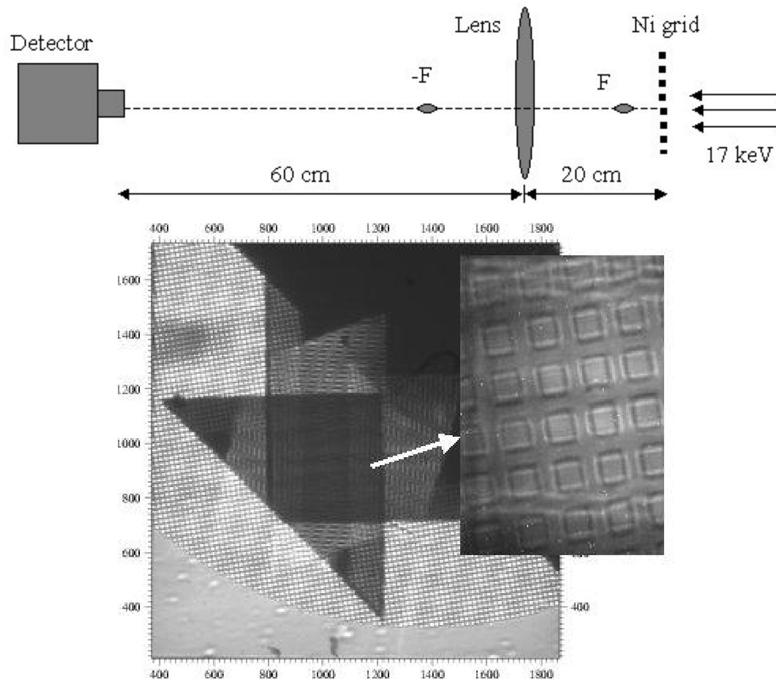

Fig. 10 Experimental setup used for full-field imaging (upper part) and recorded magnified image of the Ni grid (at the bottom).

The second test deals with the lens full field imaging of the Ni grid. The grid was illuminated with 17 keV monochromatic X-rays and was located at a distance 20 cm from the lens (Fig. 10). The 3-fold magnified image was detected at 60 cm from the lens. Figure 10 shows the X-ray image recorded with 1mm opened slits. The insert shows the lens magnified grid image. Like in the previous test the two-dimensional image is in the center and is surrounded by one-dimensional images. From the both types of imaging it is clearly seen that image is slightly aberrated but some progress in lens performance compare with previous test [7] can be evidenced.

6. RADIATION STABILITY TEST

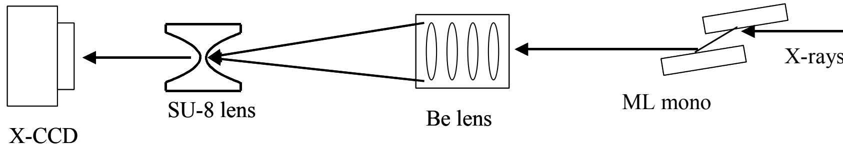

Fig. 11 Experimental setup for radiation stability test.

The radiation stability test was performed at the BM-5 ESRF beamline (Fig. 11). In order to gain in intensity flux and reduce the measurement time we used a combination of the multilayer monochromator and Be lenses as a condenser [30].

An incident X-ray energy of 13 keV was selected by using a water-cooled double multilayer monochromator with 2% bandpass [31]. The monochromatic X-rays were focused by beryllium refractive lenses to the spot of 7μm*15 μm in vertical and horizontal directions respectively with total flux of $2*10^{10}$ ph/s, that corresponds to the flux density of $2*10^{14}$ ph/s/mm^2. This value for the intensity flux is approximately 10 times higher then for the monochromatic beam at the ESRF high-β undulator beamline. Such an intense beam was impinging on the SU-8 refractive lens close to the

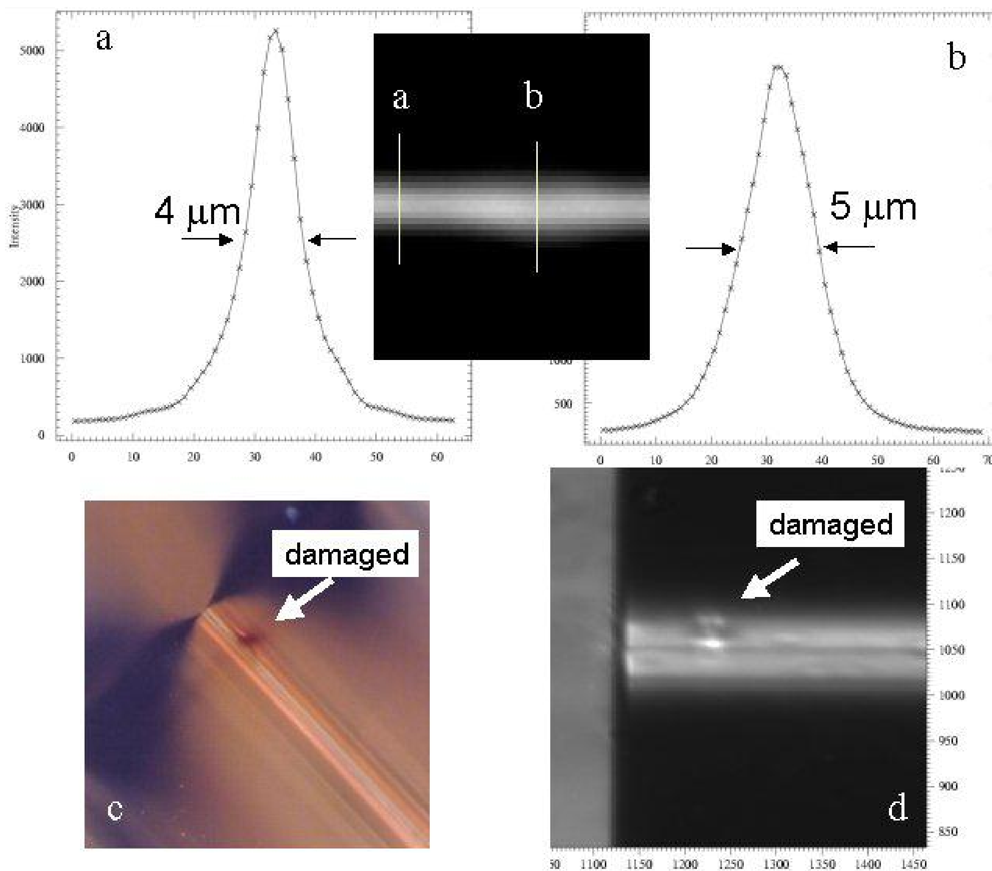

Fig. 12 Intensity distribution in the lens focal plane for the reference (a) and the damaged (b) lenses. Photo of the damaged lens taken in optical microscope (c). The X-ray image recorded with CCD camera at 30cm distance from the lens (d).

parabola apex. The SU-8 lens was consisting of 17 individual bi-concave lenses, the aperture was 340 µm, and the radius of parabola was 10 µm. At 13 keV the lens focal distance was about 19 cm. The SU-8 lens was arranged to focus X-rays in vertical direction. Focusing properties: the width of the focal line and the intensity in the spot were checked every 10 hours with X-ray CCD camera (0.67µm pixel size) by moving Be lens out of the beam. It should be noted that horizontally focused beam after Be lens (15µm) is rather smaller compare with 1 mm deep SU-8 lens. This gave us a good opportunity to record on the same image exposed and unexposed parts of the lens. After 20 hours of continuous exposure the damage of the SU-8 lens became noticeable and after 40 hours the width of the focal line was increased from 4 µm to 5 µm. The X-ray images of the focused beam of the reference and damaged areas with corresponding plots are depicted in the Fig. 12. The optical microscope photograph of the first lens in the array is shown in Fig. 12c. The dark brown spot indicates the footprint of the incoming focused beam. The damaged area of the lens is clearly seen in the X-ray image recorded with the CCD camera at a 30cm distance from the lens corresponding to 10 cm defocusing distance (Fig.12d). The observed focusing degradation can only be explained by a local degradation of the lens shape due to the radiation damage of resist cross-linking. According to our experience and rough estimates we consider the 13 keV monochromatic beam with the flux density about 10^8 ph/s/µm^2 as a “cold” beam and the local temperature increase of the SU-8 irradiated area can be neglected.

Estimations show that 20-40 hours of exposure under the conditions mentioned above are equivalent to 200-400 hours of continuous exposure at the ESRF undulator beamline with monochromatic beam, that corresponds to one month of the lens use taking into account MDT days, alignment, samples change etc. It should be pointed out that we consider here medium resolution (~ 1 µm) scheme, but in case of nanofocusing applications the lens degradation might occur rather earlier. Taking the advantage of planar technology one can design and manufacture set of tens of identical high resolution lenses on one substrate expanding the effective life time of this optical system to one year, if manufacturing technology will offer a cheap solution. In comparison with the stability test performed earlier in [7], we consider this test more adequate to real use of the lenses where pencil-like beam propagate through the lens along its optical axis. In previous test lens was exposed normally to their upper surface, lenses were poor quality and they were tested in a low-resolution mode.

7. CONCLUSION

The SU-8 planar lenses of a reasonably good quality have been manufactured at the IMT/FZK and tested at the ESRF. Sub-micrometer focusing was measured and microscopy tests were performed. A considerable volume of research has been carried out to optimize the deep lithography process for lens manufacturing. The lens performance is still limited in part by quality of manufacturing processes and further improvements and optimizations, such as a deviation of geometrical lens parameters from the designed ones, especially in depth, are still needed. We show that using coherent beam and on-line imaging detector along with the proper ray-tracing allow one to diagnose lens tiny aberrations.

The radiation test shows that lifetime of these lenses is limited at exposure doses typical for undulator monochromatic beams at the ESRF, Spring-8 and APS. It should be noted that the radiation test performed [7] is not exactly adequate to the lens working conditions, while structures were exposed normally to their upper surface, whether in the working conditions the strong dosage spreads to the first individual lenses and especially to its thinnest part. On the other hand, if technology will offer for “standard” conditions a cheap solution, disposable SU-8 (or other polymer) lenses might be widely used at the synchrotron beamlines. The LIGA technique is attractive because by utilizing standard lithography equipment the arbitrarily shaped elements can be patterned. The height of the elements up to 1mm and even deeper is can be manufactured. Dozens of lenses with different optical parameters can be formed on one substrate due to planar technology. For example, energy tunable integrated systems can be realized [18]. However, this process requires the fabrication of intermediate and working masks, possibly reducing design flexibility. If the optical requirements changed, new masks have to be obtained. A change in design can lead to a significant increase in cost and what is more, can tend to increase delay in time.

The radiation damage might be rather less at energies above 30 keV because the softer part of X-rays is cut by filters. But the presence of Sb in the resist impairs the SU-8 lens performance and makes them adequate to Al and Si lenses above 30 keV. The transition of lens technology to SU-8 resist without Sb is more preferable.

AKCNOWLEDGEMENT

We would like to thank E.Ziegler for his support during the radiation test at BM-5 beamline.

REFERENCES

1. A. Snigirev, V. Kohn, I. Snigireva and B. Lengeler, Nature (London), 384, 49, 1996.
2. A. Snigirev, V. Kohn, I. Snigireva, A. Souvorov, B. Lengeler, Applied Optics, vol. 37, No. 4, 653-662, 1998.
3. R. K. Kupka, F. Bouamrane, M.Roulliay, S. Megtert, SPIE, vol. 3680, 508-517, 1999.
4. R. K. Kupka, M. Roulliay, F. Bouamrane, S. Megtert, SPIE, vol. 3512, 398-409, 1998.
5. Ya. Zhang, T. Katoh, Ya. Kagoshima, Ju. Matui, Yo. Tsusaka, "Focusing hard X-ray with single lens", *Jpn. J. Appl. Phys*., vol. 40, L75-L77, 2001.
6. D. C. Mancini, N. A. Moldovan, R. Divan, F. de Carlo, J. Yaeger, SPIE, vol. 4783, 28-37, 2002.
7. A. Snigirev, I. Snigireva, M. Drakopoulos, V. Nazmov, E. Reznikova, S. Kuznetsov, M. Grigoriev, J. Mohr, V. Saile, SPIE, vol. 5195, 21-31, 2003.
8. V. Nazmov, L. Shabel'nikov, F.-J. Pantenburg, J. Mohr, E. Reznikova, A. Snigirev, I. Snigireva, S. Kouznetsov, M. Di Michiel, Nuclear Instruments and Methods in Physics Research, B 217, 409-416, 2004.
9. V. Nazmov, E. Reznikova, M. Boerner, J. Mohr, V. Saile, A. Snigirev, I. Snigireva, M. Di Michiel, M. Drakopoulos, R. Simon, M. Grigoriev, AIP conference proceedings, 705, 752-756, 2004.
10. V. V. Aristov, M. V. Grigoriev, S. M. Kuznetsov, L. G. Schabelnikov, V. A. Yunkin, M. Hoffmann, E. Voges, Optics Communications, 177, 33-38, 2000.
11. V. Aristov, M. Grigoriev, S. Kuznetsov, L. Shabel'nikov, V. Yunkin, T. Weitkamp, C. Rau, I. Snigireva, A. Snigirev, M. Hoffmann, E. Voges, Appl. Phys. Letters, 77, 4058, 2000.
12. V. Aristov, M. Grigoriev, S. Kuznetsov, L. Shabel'nikov, V. Yunkin, C. Rau, A. Snigirev, I. Snigireva, T. Weitkamp, M. Hoffmann, E. Voges, SPIE, vol.4145, 285, 2001.
13. I. Snigireva, A. Snigirev, C. Rau, T. Weitkamp, V. Aristov, M. Grigoriev, S. Kuznetsov, L. Shabelnikov, V. Yunkin, M. Hoffmann, E. Voges, Nuclear Instruments & Methods, A 467-468, 982, 2001.
14. M. Grigoriev, L. Shabelnikov, V. Yunkin, A. Snigirev, I. Snigireva, M. Di Michiel, S. Kuznetsov, M. Hoffmann, E. Voges, SPIE, vol. 4501, 185, 2001.
15. I. Snigireva, A. Snigirev, S. Kuznetsov, C. Rau, T. Weitkamp, L. Shabelnikov, M. Grigoriev, V. Yunkin, M. Hoffmann, E. Voges, SPIE, vol. 4499, 64, 2001.
16. I. Snigireva, M. Grigoriev, L. Shabelnikov, V. Yunkin, A. Snigirev, S. Kuznetsov, M. Di Michiel, M. Hoffmann, E. Voges, SPIE, vol. 4783, 19-27, 2002.
17. C. G. Schroer, M. Kuhlmann, U. T. Hunger, T. F. Gunsler, O. Kurapova, S. Feste, F. Frehse, B. Lengeler, M. Drakopoulos, A. Somogyi, A. Simionovici, A. Snigirev, I. Snigireva, C. Schug, W. H. Schroder, Appl. Phys. Letters, 82(9), 1485-1487, 2003.
18. I. Snigireva, A. Snigirev, V. Yunkin, M. Drakopoulos, M. Grigoriev, S. Kuznetsov, M. Chukalina, M Hoffmann, D. Nuesse, E. Voges, AIP conference proceedings, 705, 708-712, 2004.
19. C. G. Schroer, M. Kuhlmann, U. T. Hunger, T. F. Gunsler, O. Kurapova, S. Feste, B. Lengeler, M. Drakopoulos, A Somogyi, A. S. Simionovici, A. Snigirev, I. Snigireva, AIP conference proceedings, 705, 740-744, 2004.
20. A. Snigirev, V. Yunkin, I. Snigireva, M. Di Michiel, M. Drakopoulos, S. Kouznetsov, L. Shabelnikov, M. Grigoriev, V. Ralchenko, I. Sychov, M. Hoffmann, E. Voges, SPIE, vol. 4783, 1-9, 2002.
21. B. Nohammer, J. Hoszowska, A. Freund, C. David, Journal of Synchrotron Radiation, 10, 168-171, 2003.
22. A. Artemiev, A. Snigirev, V. Kohn, I. Snigireva, N. Artemiev, M. Grigoriev, S. Peredkov, L. Glikin, M. Levtonov, V. Kvardakov, À. Zabelin, A. Maevsky, this proceedings.
23. M. Drakopoulos, J. Zegenhagen, A. Snigirev, I. Snigireva, M. Hauser, K. Eberl, V. Aristov, L. Shabelnikov, V. Yunkin, Appl. Phys. Letters, 81(12), 2279-2281, 2002.
24. M. Drakopoulos, J. Zegenhagen, T.-L. Lee, A. Snigirev, I. Snigireva, V. Cimalla, O. Ambacher, J. Phys. D: Appl. Phys., 36, A214-A216, 2003.
25. M. Drakopoulos, J. Zegenhagen, A. Snigirev, I. Snigireva, "Microscopy with X-ray standing waves", Synchrotron Radiation News, vol. 17, No. 3, 37-42, 2004.
26. J. M. Shaw, J. D. Gelorme, N. C. LaBianca, W. E. Conley, S. J. Holmes, IBM J. Res. Develop., vol. 41, No. ½, 81-94, 1997.
27. V. Kohn, I. Snigireva, A. Snigirev, Optics Communications, vol. 216, 247-260, 2003.
28. W. Ehrfeld, P. Bley, F. Gotz, J. Mohr, D. Munchmeyer, W. Schelb, J. Vac. Sci Tech. B6, 178-182,1988.
29. W. Menz, J. Mohr, "Mikrosystemtechnik fur Ingenieure", Wiley, Weinheim, 1997.
30. B. Lengeler, C. G. Schroer, M. Kuhlmann, B. Benner, T. F. Gunsler, A. Somogyi, A. Snigirev, I. Snigireva, AIP conference proceedings, 705, 748-752, 2004.
31. T. Bigault, E. Ziegler, C. Morawe, R. Hustache, J.-Y. Massonnat, G. Rostaing, SPIE, vol. 5195, 12-20,2003.